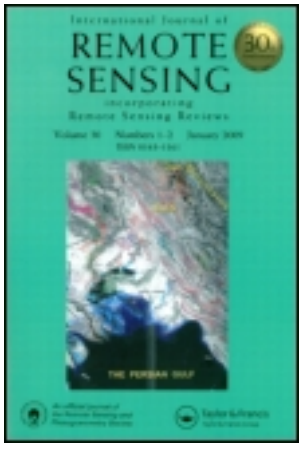

International Journal of Remote Sensing

Publication details, including instructions for authors and subscription information:
http://www.tandfonline.com/loi/tres20

Using the normalized peak area of remote sensing reflectance in the near-infrared region to estimate total suspended matter

W. Ma [a], Q. Xing [a], C. Chen [b], Y. Zhang [c], D. Yu [a] & P. Shi [a]

[a] Yantai Institute of Coastal Zone Research, Chinese Academy of Sciences, Yantai, 264003, China

[b] Laboratory for Tropical Marine Environmental Dynamics (LED), South China Sea Institute of Oceanology, Chinese Academy of Sciences, Guangzhou, 510301, China

[c] Institute of Space and Earth Information Science, Chinese University of Hong Kong, Shatin, Hong Kong, China

Available online: 11 Aug 2011

To cite this article: W. Ma, Q. Xing, C. Chen, Y. Zhang, D. Yu & P. Shi (2011): Using the normalized peak area of remote sensing reflectance in the near-infrared region to estimate total suspended matter, International Journal of Remote Sensing, 32:22, 7479-7486

To link to this article: http://dx.doi.org/10.1080/01431161.2010.524673

International Journal of Remote Sensing
Vol. 32, No. 22, 20 November 2011, 7479–7486

Taylor & Francis
Taylor & Francis Group

Using the normalized peak area of remote sensing reflectance in the near-infrared region to estimate total suspended matter

W. MA†, Q. XING*†, C. CHEN‡, Y. ZHANG§, D. YU† and P. SHI†
†Yantai Institute of Coastal Zone Research, Chinese Academy of Sciences, Yantai 264003, China
‡Laboratory for Tropical Marine Environmental Dynamics (LED), South China Sea Institute of Oceanology, Chinese Academy of Sciences, Guangzhou 510301, China
§Institute of Space and Earth Information Science, Chinese University of Hong Kong, Shatin, Hong Kong, China

(*Received 6 May 2009; in final form 2 November 2009*)

The normalized peak area (NPA) of remote-sensing reflectance (R_{rs}) in the near-infrared region was used to estimate the concentration of total suspended matter (C_{TSM}) in coastal waters. A linear regression model between C_{TSM} and S_{NPA} ($R^2 = 0.83$) was established, where S_{NPA} is the area encompassed by the reflectance curve and the straight line between wavelengths 768 and 840 nm where there is a maximum of R_{rs} near 715 nm. In the Pearl River estuary of South China, this NPA model performed better than other single-band and multi-band regression models, with a root mean square error (RMSE) of 4.07 mg l^{-1}. This model may be widely applied to *in situ* measurements of TSM.

1. Introduction

Total suspended matter (TSM) is one of the key colour-producing agents in water. A number of remote-sensing models have been proposed to estimate TSM. Hoogenboom *et al*. (1998) proposed a matrix model to retrieve the concentration of TSM (C_{TSM}) from underwater irradiance. Using the near-infrared bands, Moore (1980) obtained C_{TSM} on the basis of the bidirectional reflectance distribution functions (BDRFs) on the water surface. Based on the forward and inverse modelling of light radiation transfer, Dekker *et al*. (2001, 2002) developed an analytical algorithm to estimate C_{TSM}; this model could be applied to Landsat Thematic Mapper (TM) and Satellite Pour l'Observation de la Terre (SPOT) images. On the basis of the spectral characteristics of *in situ* spectra and remote-sensing images, Binding *et al*. (2003) obtained retrieval models of water quality parameters including C_{TSM}. In the study of Teodoro *et al*. (2007b), the retrieval accuracy of a multiple-band regression model was better than that of an artificial neural network (ANN) model. Schiebe *et al*. (1992) and Harrington *et al*. (1992) proposed an exponential function to describe the relationship between extra-atmospheric reflectance and suspended sediment concentration on the basis of Landsat Multispectral Scanner (MSS) data and *in situ* suspended sediment

*Corresponding author. Email: qgxing@yahoo.com

International Journal of Remote Sensing
ISSN 0143-1161 print/ISSN 1366-5901 online © 2011 Taylor & Francis
http://www.tandf.co.uk/journals
http://dx.doi.org/10.1080/01431161.2010.524673

concentrations; more recently, this work has been extended to retrieve chlorophyll-*a* concentration (Dall'Olmo *et al*. 2003).

For the estimation of C_{TSM}, empirical algorithms usually have relatively higher retrieval precision. Nevertheless, they are often restricted by specific temporal and spatial conditions. Analytical algorithms adopt bio-optical models for retrieving C_{TSM} on the basis of the inherent and apparent optical properties of water constituents. In many cases, analytical models have a poor performance because of difficulties in obtaining accurate absorption and backscattering coefficients from optically complex Case-II waters. Semi-analytical models are commonly used to retrieve C_{TSM} because they are simpler and have higher retrieval accuracy than the empirical and analytical algorithms. However, most of the semi-analytical algorithms developed so far also have temporal and spatial restrictions, and cannot be used widely in different regions. It is therefore important to find a TSM retrieval method that can be widely used in different areas with varied environmental factors.

In the visible and near-infrared spectral regions, and especially in the near-infrared, most of the backscattering is caused by suspended matter in comparison to other major colour-producing constituents in water (Ruddick *et al*. 2006, Teodoro *et al.* 2007a). Mahtab *et al*. (1998) investigated the responses of remote-sensing reflectance (R_{rs}) to different C_{TSM} according to the simulated spectra, and concluded that TM band 4 (TM4) was the best band for retrieving C_{TSM}. Gitelson *et al*. (1993) pointed out that the reflectance at 700–900 nm was sensitive to TSM, and these bands were the best for retrieving C_{TSM} from reflectance. The near-infrared region was therefore chosen in the current work for an effective model for retrieving C_{TSM} according to the optical properties of suspended matter in water.

2. Methods

2.1 In situ *measurements and data preprocessing*

Twenty-eight water samples were collected from two different cruises, on 6 and 21 December 2006, respectively (see figure 1 for study area and sampling sites). A portable field spectroradiometer (SD2000 from Ocean Optics Inc., Dunedin, FL, USA) was used to measure the above-water R_{rs} (Shi *et al*. 2007, Xing *et al*. 2008). The R_{rs} spectra were resampled at a spectral resolution of 1 nm, and the region between 740 and 875 nm (figure 2) was chosen for analysing the spectral properties. The C_{TSM} was determined by the weighing method. The water samples were filtered through pre-weighed Whatman polycarbonate membrane filters (GE Healthcare, UK) with a nominal pore diameter of 0.20 μm, and then the filters containing particles were dried at 60°C until there was no change in weight. The quantities of TSM were obtained by subtracting the initial weights of the filters from the weights after drying, and the TSM concentrations were calculated according to the TSM quantities and the volumes of the filtered water samples.

2.2 *Calculation of normalized peak area*

In the near-infrared region of each R_{rs} spectrum (figure 2), one peak and two troughs could be seen at the wavelengths 815, 768 and 840 nm, respectively. The peak may be obtained because there is less water absorption at 815 nm compared with 768 and 840 nm (Palmer and Williams 1974). Atmospheric absorption at 810–830 nm (Xing 2007) together with the fluorescence (Xing *et al*. 2008) and/or Raman scattering in water

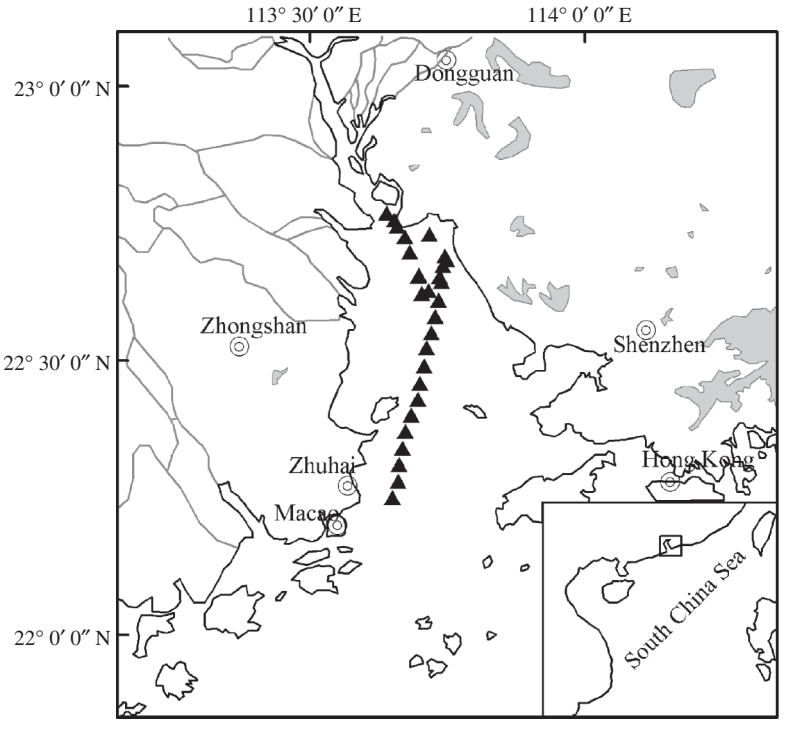

Figure 1. Sampling sites in the field campaign conducted at the Pearl River estuary of South China in December 2006.

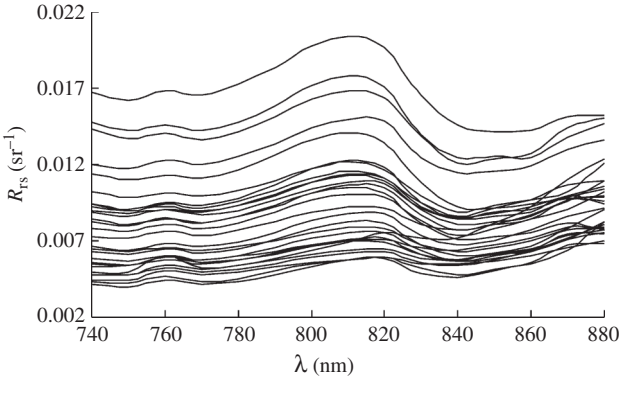

Figure 2. Large variations in the near-infrared R_{rs}. One peak and two troughs are located near 815, 768 and 840 nm, respectively.

may also contribute to the peak. This issue, however, is beyond the scope of the present study and will be explored separately in a further study. Based on this feature of an R_{rs} peak in the near-infrared region, a conceptual model of the normalized peak area (NPA) (figure 3) was proposed as follows: (1) calculate the area under the R_{rs} curve at 768–840 nm; and (2) obtain the NPA by subtracting the area under the straight line

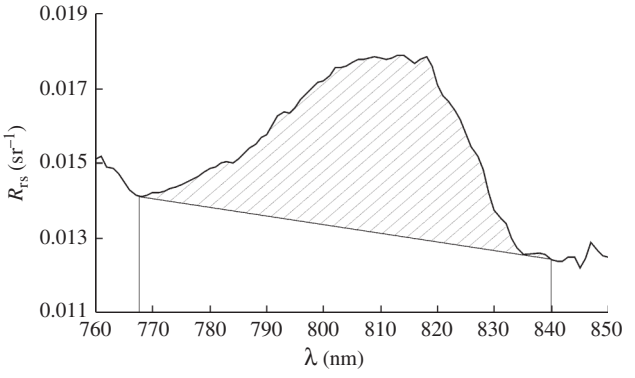

Figure 3. Conceptual model of the normalized peak area (NPA) in the near-infrared region (see the shaded area).

between 768 and 840 nm from the area calculated in step 1. Hence the calculation of the NPA is obtained from:

$$S_{\mathrm{NPA}} = \sum_{768}^{840} [R_{\mathrm{rs}}(\lambda)B] - \frac{[R_{\mathrm{rs}}(768) + R_{\mathrm{rs}}(840)] \times (840 - 768)}{2}, \tag{1}$$

where S_{NPA} is the normalized peak area (sr^{-1} nm), $R_{\mathrm{rs}}(\lambda)$ is the remote sensing reflectance at wavelength λ (sr^{-1}) and B is the wavelength interval between two adjacent bands (1 nm in this study). Using this method, S_{NPA} values for the 28 water samples were calculated.

Reed *et al.* (1994) used a similar strategy, using a time-integrated normalized difference vegetation index (NDVI) during the plants' growing season as an important surrogate measure of ecosystem characteristics. In this study, a wavelength-integrated R_{rs} index was used to extract C_{TSM}. Fresnel effects should be considered in the measurements of the above-water reflectance. The skylight reflectance spectrum is generally flat at 750–850 nm (Xing 2007), so the normalizing method in the NPA model can be expected to reduce the impact of reflected skylight at the water surface.

2.3 *Estimation of TSM concentration using NPA*

As shown in figure 4, C_{TSM} values are linearly proportional to S_{NPA}, with a coefficient of determination (R^2) of 0.83, so a simple linear regression model (equation (2)) was established to retrieve C_{TSM} from S_{NPA}:

$$C_{\mathrm{TSM}} = 184.7 \times S_{\mathrm{NPA}} + 3.5539, \tag{2}$$

where C_{TSM} is the retrieved TSM concentration. The root mean square error (RMSE) between the retrieved values and the *in situ* measured concentrations was 4.07 mg l^{-1}. When the concentrations were lower than 30 mg l^{-1} (figure 4), there was a lower correlation between C_{TSM} and S_{NPA}. This may be partly attributable to the larger error that can be expected in measurements of low TSM concentrations when the weighing method is used.

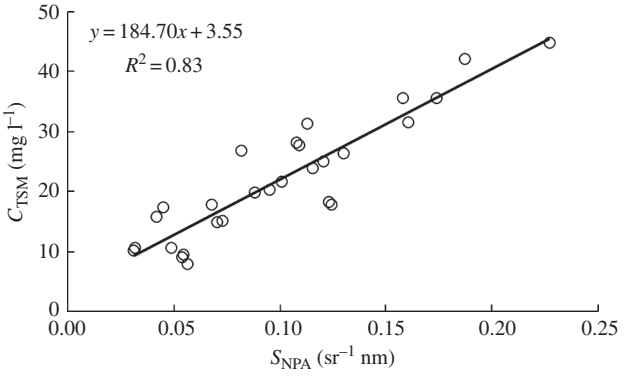

Figure 4. Relationship between C_{TSM} and S_{NPA}.

3. Discussion

3.1 *Comparison with other retrieval algorithms*

To examine the retrieval precision of the NPA algorithm, single-band models and multiple-band models were used for comparison.

3.1.1 Single-band models. Figure 2 presents all the 28 R_{rs} spectra measured in the field campaign. The R_{rs} near 810 nm averaged 0.010 sr^{-1}, with a standard deviation of 0.004 sr^{-1}. The signals of R_{rs} are strong in the near-infrared region, and could not be neglected as is usual with R_{rs} spectra from Case-I waters. On the contrary, the strong reflection is one of the important spectral characteristics in turbid waters (Case-II), and may be used to retrieve the TSM concentration. The R_{rs} values near 810 nm ranged from 0.005 to 0.020 sr^{-1}, and generally increased with an increase in TSM concentration (7.96–44.86 mg l^{-1}); for example, the top curve in figure 2 corresponds to the largest TSM concentration (i.e. 44.86 mg l^{-1}) and the lowest curve to a concentration of 8.96 mg l^{-1} (close to the lowest value of 7.96 mg l^{-1}). In addition, the peak appeared to be more prominent with increasing TSM concentration.

Lv *et al*. (2005) found that $R_{rs}(810)$ was sensitive to C_{TSM} in their work at the Tai Lake waters (typical inland Case-II waters), and that the linear regression model was the best among the regression models. However, in our work at the Pearl River estuary, the best correlation between single bands and C_{TSM} was found at 740 nm, and the corresponding maximum of R^2 was 0.83. With the single-band model (equation (3)), the precision of TSM retrieval in the Pearl River estuary was 4.07 mg l^{-1} in the RMSE, close to that of the NPA model. However, this also means that the single-band model may be not robust: for different waters, we have to choose a different band. Because the signals come from many sources, we know that the variations in R_{rs} are not only related to the TSM concentration. There was a curve-intersecting phenomenon in R_{rs} (figure 2), especially at wavelengths longer than 840 nm, which might also be caused by the effects of ambient light and complex water constituents.

$$C_{TSM} = 2740.9 \times R_{rs}(740) - 0.1704. \quad (3)$$

3.1.2 Multiple-band models. Multiple-band models link different bands and/or band combinations to TSM concentrations. A popular multiple-band model with high precision was originally applied to retrieve C_{TSM} at the Mediterranean Sea by Tassan (1994); this model has been widely applied to coastal waters to retrieve TSM. Tang *et al*. (2004) modified the Tassan model and applied it to the Yellow Sea and the East China Sea for the retrieval of TSM. In this study, the improved linear model, as shown in equation (4), was tested for comparison:

$$\log_{10}(C_{\mathrm{TSM}}) = 1.106 + 11.035 \times [R_{\mathrm{rs}}(555) + R_{\mathrm{rs}}(670)] - 0.685 \times \left[\frac{R_{\mathrm{rs}}(490)}{R_{\mathrm{rs}}(555)}\right]. \quad (4)$$

The coefficient of determination of the improved linear model was 0.75, which was lower than that in the NPA model. In the test of retrieval, the NPA model showed better performance, compared with the RMSE of 6.11 mg l^{-1} from the improved Tassan model.

Finally, the reflectance peak line height model was also used to validate the NPA model. As mentioned earlier, there was one reflectance peak near 815 nm (figure 2) that could be used to retrieve C_{TSM}. For details of the peak line height, refer to Liu *et al.* (2004). A regression model (equation (5)), was applied to retrieve C_{TSM}:

$$C_{\mathrm{TSM}} = 7157.7 H_{R_{\mathrm{rs}}} + 5.1916, \quad (5)$$

where $H_{R_{\mathrm{rs}}}$ is the peak line height at 815 nm. The coefficient of determination ($R^2 = 0.82$) and the RMSE (4.16 mg l^{-1}) were both close to those from the NPA model. This is because the two models have a similar strategy of using the peak R_{rs} near 815 nm together with the R_{rs} at the wings (768 and 840 nm, respectively). We should note that the NPA model is a multi-band model too.

3.2 *Retrieval precision*

The retrieved C_{TSM} values using the NPA model (presented by equations (1) and (2)) were in good agreement with the *in situ* measurements (RMSE = 4.07 mg l^{-1}), with an R^2 of 0.83. The NPA model showed better performance than the other single-band or multi-band models. The water salinity and temperature have much more influence on absorption and reflection in the near-infrared region than in the visible region (Pegau *et al.* 1997), so changes in these parameters may bring additional errors. Compared with other retrieval models of TSM, all the above-mentioned models had relatively higher retrieval precisions except for the improved Tassan model. In general, the NPA's performance was comparable to or even better than those popular models used in this study. The NPA model may be the new method of choice in the retrieval of TSM concentration.

4. Conclusions

In the visible spectral region, the ideal wavelengths for TSM retrieval are not robust in different regions because of the impact of phytoplankton pigments and coloured dissolved organic matter (CDOM). However, the characteristic wavelengths responding to TSM in the near-infrared region are relatively fixed, in comparison to those in the visible region (Teodoro *et al.* 2007a). Taking into account the spectral properties

of TSM in the near-infrared region, an NPA model was proposed to retrieve C_{TSM}. The NPA was calculated according to the peak $R_{rs}(815)$ and two troughs $R_{rs}(768)$ and $R_{rs}(840)$. Our study in the Pearl River estuary has demonstrated that the NPA method is an efficient retrieval algorithm for TSM on the basis of a local empirical model.

However, the reasons for the peak near 815 nm are not fully known, and will be investigated in future studies. TSM concentrations may vary by season and region. Xing (2007) reported that the TSM concentration can be up to 150 mg l^{-1} at the river channel near the Pearl River estuary. The current NPA model was obtained for limited TSM concentrations (figure 4), that is less than 50 mg l^{-1}, and so it needs to be validated for a wide range of TSM concentrations.

Acknowledgements

This work received support from China National 863 project (No. 2009AA12Z135), the Chinese Academy of Sciences (No. KZCX2-YW-Q07-01) and the direct grants from the Chinese University of Hong Kong (No. 2020928) and Hong Kong General Research Fund (RGC No. CUHK454909). Support from CNRS and CNES, France, through funding, and from the project COULCOT in the framework of the TOSCA programme is also acknowledged. We thank two anonymous reviewers for their helpful comments.

References

Binding, C.E., Bowers, D.G. and Mitchelson-Jacob, E.G., 2003, An algorithm for the retrieval of suspended sediment concentrations in the Irish Sea from SeaWiFS ocean colour satellite imagery. *International Journal of Remote Sensing*, **24**, pp. 3791–3806.

Dall'Olmo, G., Gitelson, A.A. and Rundquist, D.C., 2003, Towards a unified approach for remote estimation of chlorophyll-a in both terrestrial vegetation and turbid productive waters. *Geophysical Research Letters*, **30**, pp. 1938–1941.

Dekker, A.G., Vos, R.J. and Peters, S.W.M., 2001, Comparison of remote sensing data, model results and in situ data for total suspended matter (TSM) in the southern Frisian lakes. *Science of the Total Environment*, **268**, pp. 197–214.

Dekker, A.G., Vos, R.J. and Peters, S.W.M., 2002, Analytical algorithms for lake water TSM estimation for retrospective analyses of TM and SPOT sensor data. *International Journal of Remote Sensing*, **23**, pp. 15–35.

Gitelson, A., Garbuzov, G., Szilagyi, F., Mittenzwey, K.H., Karnieli, A. and Kaiser, A., 1993, Quantitative remote sensing methods for real-time monitoring of inland waters quality. *International Journal of Remote Sensing*, **14**, pp. 1269–1295.

Harrington, J.J., Schiebe, F.R. and Nix, J.F., 1992, Remote sensing of Lake Chicot, Arkansas: monitoring suspended sediments, turbidity, and secchi depth with Landsat MSS data. *Remote Sensing of Environment*, **39**, pp. 15–27.

Hoogenboom, H.J., Dekker, A.G. and Althuis, I.A., 1998, Simulation of AVIRIS sensitivity for detecting chlorophyll over coastal and inland waters – a review. *Remote Sensing of Environment*, **65**, pp. 333–340.

Liu, T., Kuang, D. and Yin, Q., 2004, Study on hyperspectral quantitative model of concentrations for chlorophyll-a of alga and suspended particles in Tai Lake. *Journal of Infrared and Millimeter Waves*, **23**, pp. 11–15.

Lv, H., Li, X. and Jiang, N., 2005, Estimation of suspended solids concentration in Lake Taihu using spectral reflectance and simulated MERIS. *Journal of Lake Science*, **17**, pp. 104–109.

Mahtab, A.L., Runquist, D.C., Han, L.H. and Kuzila, M.S., 1998, Estimation of suspended sediment concentration in water using integrated surface reflectance. *Geocarto International*, **13**, pp. 11–15.

Moore, G.K., 1980, Satellite remote sensing of water turbidity. *Hydrological Sciences Bulletin*, **25**, pp. 407–421.

Palmer, K.F. and Williams, D., 1974, Optical properties of water in the near infrared. *Journal of the Optical Society of America*, **64**, pp. 1107–1110.

Pegau, W.S., Gray, D. and Zaneveld, J.R.V., 1997, Absorption and attenuation of visible and near-infrared light in water: dependence on temperature and salinity. *Applied Optics*, **36**, pp. 6035–6046.

Reed, B.C., Brown, J.F., VanderZee, D., Loveland, T.R., Merchant, J.W. and Ohlen, D.O., 1994, Measuring phenological variability from satellite imagery. *Journal of Vegetation Science*, **5**, pp. 703–714.

Ruddick, K.G., Cauwer, V.D., Park, Y.J. and Moore, G., 2006, Seaborne measurements of near infrared water-leaving reflectance: the similarity spectrum for turbid waters. *Limnology and Oceanography*, **51**, pp. 1167–1179.

Schiebe, F.R., Harrington, J.J. and Ritchie, J.C., 1992, Remote sensing of suspended sediments: the Lake Chicot, Arkansas project. *International Journal of Remote Sensing*, **13**, pp. 1487–1509.

Shi, H., Xing, Q., Chen, C., Shi, P. and Tang, S., 2007, Using second-derivative spectrum to estimate chlorophyll-a concentration in turbid estuarine waters. *Proceedings of SPIE*, **6790**, 679032.

Tang, J., Wang, X., Song, Q., Li, T., Chen, J., Huang, H. and Ren, J., 2004, The statistic inversion algorithms of water constituents for the Huanghai Sea and the East China Sea. *Acta Oceanologica Sinica*, **23**, pp. 617–626.

Tassan, S., 1994, Local algorithms using SeaWiFS data for the retrieval of phytoplankton, pigments, suspended sediments, and yellow substance in coastal waters. *Applied Optics*, **33**, pp. 2369–2378.

Teodoro, A.C., Marcal, A.R.S. and Veloso-Gomes, F., 2007a, Correlation analysis of water wave reflectance and local TSM concentrations in the breaking zone with remote sensing techniques. *Journal of Coastal Research*, **23**, pp. 1491–1497.

Teodoro, A.C., Veloso-Gomes, F. and Goncalves, H., 2007b, Retrieving TSM concentration from multispectral satellite data by multiple regression and artificial neural networks. *IEEE Transactions on Geoscience and Remote Sensing*, **45**, pp. 1342–1350.

Xing, Q., 2007, Retrieval of water quality in the Pearl River estuary using hyperspectral techniques. PhD thesis, South China Sea Institute of Oceanology, Graduate University of the Chinese Academy of Sciences, China.

Xing, Q., Chen, C., Shi, H., Shi, P. and Zhang, Y., 2008, Estimation of chlorophyll-a concentrations in the Pearl River estuary using in-situ hyperspectral data: a case study. *Marine Technology Society Journal*, **42**, pp. 22–27.